

## ARTICLE OPEN



## Clinical Studies

# AHRR and SFRP2 in primary versus recurrent high-grade serous ovarian carcinoma and their prognostic implication

Nanna Monjé<sup>1,15</sup>, Mihnea P. Dragomir<sup>1,2,3,15</sup>, Bruno V. Sinn<sup>1</sup>, Inga Hoffmann<sup>1</sup>, Anuar Makhmut<sup>4</sup>, Tincy Simon<sup>1</sup>, Catarina A. Kunze<sup>1</sup>, Jana Ihlow<sup>1,3</sup>, Wolfgang D. Schmitt<sup>1</sup>, Jonathan Pohl<sup>1</sup>, Iris Piwonski<sup>1</sup>, Sofya Marchenko<sup>1</sup>, Carlotta Keunecke<sup>5</sup>, Teodor G. Calina<sup>6</sup>, Francesca Tiso<sup>7,8</sup>, Hagen Kulbe<sup>5</sup>, Caroline Kreuzinger<sup>9</sup>, Dan Cacsire Castillo-Tong<sup>9</sup>, Jalid Sehoul<sup>2,3,5</sup>, Elena I. Braicu<sup>2,3,5</sup>, Carsten Denkert<sup>10</sup>, Silvia Darb-Esfahani<sup>11</sup>, Kirsten Kübler<sup>2,7,8,12,13</sup>, David Capper<sup>2,14</sup>, Fabian Coscia<sup>4</sup>, Markus Morkel<sup>1,2,3</sup>, David Horst<sup>1,2,3</sup>, Christine Sers<sup>1,2,3,16</sup> and Eliane T. Taube<sup>1,16</sup>✉

© The Author(s) 2024

**BACKGROUND:** The aim of this study was to analyse transcriptomic differences between primary and recurrent high-grade serous ovarian carcinoma (HGSOC) to identify prognostic biomarkers.

**METHODS:** We analysed 19 paired primary and recurrent HGSOC samples using targeted RNA sequencing. We selected the best candidates using in silico survival and pathway analysis and validated the biomarkers using immunohistochemistry on a cohort of 44 paired samples, an additional cohort of 504 primary HGSOCs and explored their function.

**RESULTS:** We identified 233 differential expressed genes. Twenty-three showed a significant prognostic value for PFS and OS in silico. Seven markers (*AHRR*, *COL5A2*, *FABP4*, *HMGCS2*, *ITGAS*, *SFRP2* and *WNT9B*) were chosen for validation at the protein level. *AHRR* expression was higher in primary tumours ( $p < 0.0001$ ) and correlated with better patient survival ( $p < 0.05$ ). Stromal *SFRP2* expression was higher in recurrent samples ( $p = 0.009$ ) and protein expression in primary tumours was associated with worse patient survival ( $p = 0.022$ ). In multivariate analysis, tumour *AHRR* and *SFRP2* remained independent prognostic markers. In vitro studies supported the anti-tumorigenic role of *AHRR* and the oncogenic function of *SFRP2*.

**CONCLUSIONS:** Our results underline the relevance of *AHRR* and *SFRP2* proteins in aryl-hydrocarbon receptor and Wnt-signalling, respectively, and might lead to establishing them as biomarkers in HGSOC.

British Journal of Cancer (2024) 130:1249–1260; <https://doi.org/10.1038/s41416-023-02550-1>

## INTRODUCTION

Ovarian cancer (OC) is the fifth leading cause of cancer death for women in Western countries [1]. Among several histological subtypes, high-grade-serous ovarian carcinoma (HGSOC) is the most common one, often diagnosed at a late stage when the tumour has already spread within the abdominal cavity [2]. Consequently, HGSOC accounts for the highest number of deaths among ovarian cancer patients and 5-year survival is as low as 43% [3]. A major setback for successful treatment of OC patients is relapse of primary tubo-ovarian carcinomas, which occurs after primary response to therapy and is experienced in

approximately 80% of patients. The median time from primary diagnosis to recurrence is only 16 months [4]. As these recurrences often become resistant to conventional therapies, treatment options are limited and overall life expectancy for these patients is short.

Despite its immense clinical importance, data on treatment resistance mechanisms and the unique biology of relapsed HGSOC is still sparse. An explanation might be the difficulty in obtaining matched primary and recurrent samples, as surgery is not generally performed in the relapsed stage and candidates for surgical treatment must be chosen conscientiously [5].

<sup>1</sup>Charité—Universitätsmedizin Berlin, Corporate Member of Freie Universität Berlin and Humboldt-Universität zu Berlin, Institute of Pathology, Charitéplatz 1, 10117 Berlin, Germany. <sup>2</sup>German Cancer Consortium (DKTK), Partner Site Berlin, and German Cancer Research Center (DKFZ), Heidelberg, Germany. <sup>3</sup>Berlin Institute of Health (BIH), Berlin, Germany. <sup>4</sup>Max-Delbrück-Center for Molecular Medicine in the Helmholtz Association (MDC), Spatial Proteomics Group, Berlin, Germany. <sup>5</sup>Charité—Universitätsmedizin Berlin, corporate member of Freie Universität Berlin and Humboldt-Universität zu Berlin, Department for Gynecology with the Center for Oncologic Surgery Charité Campus Virchow-Klinikum, Charitéplatz 1, 10117 Berlin, Germany. <sup>6</sup>TGC Ventures UG, Berlin, Germany. <sup>7</sup>Center of Functional Genomics, Berlin Institute of Health at Charité—Universitätsmedizin Berlin, Charitéplatz 1, 10117 Berlin, Germany. <sup>8</sup>Department of Hematology, Oncology and Cancer Immunology, Charité—Universitätsmedizin Berlin, corporate member of Freie Universität Berlin and Humboldt-Universität zu Berlin, Hindenburgdamm 30, 12203 Berlin, Germany. <sup>9</sup>Translational Gynecology Group, Department of Obstetrics and Gynecology, Comprehensive Cancer Center, Medical University of Vienna, Vienna, Austria. <sup>10</sup>Institute of Pathology, University Hospital Gießen and Marburg, Marburg, Germany. <sup>11</sup>Institute of Pathology, Berlin-Spandau, Stadtrandstraße 555, 13589 Berlin, Germany. <sup>12</sup>Cancer Program, Broad Institute of MIT and Harvard, Cambridge, MA, USA. <sup>13</sup>Center for Cancer Research, Massachusetts General Hospital, Harvard Medical School Teaching Hospital, Charlestown, MA, USA. <sup>14</sup>Department of Neuropathology, Charité—Universitätsmedizin Berlin, Corporate Member of Freie Universität Berlin, Humboldt-Universität zu Berlin, Berlin, Germany. <sup>15</sup>These authors contributed equally: Nanna Monjé, Mihnea P. Dragomir. <sup>16</sup>These authors jointly supervised this work: Christine Sers, Eliane T. Taube. ✉email: [eliane.taube@charite.de](mailto:eliane.taube@charite.de)

Received: 4 December 2022 Revised: 3 December 2023 Accepted: 11 December 2023

Published online: 9 February 2024

Recent research from transnational consortia addressed these problems [6–8]. It seems that apart from the known dysregulation of homologous recombination deficiency (HRD) and *TP53*, both of which play an important role in tumour initiation of HGSOc [9, 10], additional molecular mechanisms, for example, the upregulation of a therapy resistance-related drug efflux pump (MDR1) become important for tumour preservation after primary chemotherapy [8]. Analyses on the temporal heterogeneity in immune response [6, 11, 12] and angiogenesis [13] in recurrent HGSOc concentrated on the evaluation of specific immunohistochemically (IHC) detectable markers. However, to date, there has been no exploratory analysis of differentially expressed genes in the recurrence of HGSOc that includes protein-based validation.

We aimed to discover molecules that mark the progression from primary to recurrent samples under the assumption that these markers would be more pronounced in recurrences. Therefore, we analysed signalling pathways involved in the process of tumour recurrence. We further wondered if the detected differentially expressed markers were merely an adaptation to tumour progression or if their initial presentation in the primary tumour would also indicate prognostic potential and they could thus serve as biomarkers. We focused on the prognostic impact of a small subset of promising candidates in a cohort of 504 primary HGSOc samples with well-annotated survival data to assess their clinical utility for patient stratification and survival prediction. AHRH and SFRP2 were demonstrated to be consistently clinically relevant markers throughout these analyses and exploratory studies were performed to understand their upstream regulation and downstream function.

## METHODS

### Patient Cohort

Three independent patient collectives were included in this study. The first one consists of paired primary and recurrent HGSOc (PRI-REC-Cohort; Screening ( $n = 19$ ) and validation cohort ( $n = 44$ )) and is complemented by a second one of primary tumours (PRI-Cohort; Survival cohort ( $n = 504$ )), and an additional cohort served for analysis of HRD status ( $n = 66$ ).

The PRI-REC-Cohort consists of HGSOc patients who were treated between 2001 and 2015 at the Department of Gynaecology, Charité University Hospital Berlin. From these patients, paired tissue samples of their primary and recurrent lesions were available, which have been examined at the Institute of Pathology, Charité University Hospital Berlin. Patients were recruited in the OCTIPS project (Ovarian Cancer Therapy—Innovative Models Prolong Survival, [www.octips.eu](http://www.octips.eu)) and samples underwent central pathological review. Out of a total of 107 samples, cases were excluded if paired samples were not available ( $n = 22$ ), samples were histologically inappropriate for our study ( $n = 13$ ), or patients had already received neoadjuvant chemotherapy (NACT) ( $n = 10$ ). After IHC evaluation, an additional 18 pairs had to be excluded: in five cases, TMA tissue of either the primary or the relapse samples was of insufficient quality and 13 pairs were excluded retrospectively because of falsely positive negative controls. Thus, 44 paired samples were available for IHC analyses (Supplementary Fig. 1a).

The PRI-Cohort consists of patients who likewise were treated and diagnosed at Charité and includes primary HGSOc specimens from patients followed between 2000 and 2021. Staining of p53 was used as an additional quality control for histotype [14]. In total, 504 patient samples could be included in our study (survival cohort), as they were considered eligible after reviewing for the above-mentioned inclusion and exclusion criteria (Supplementary Fig. 1b).

The HRD cohort consists of 66 HGSOc patients with mutated *TP53* (determined in 61 cases by immunohistochemical expression pattern and in 5 cases by molecular analysis). In 60 patients HRD status was determined using the HRD Plus Test Myriad Genetic Laboratories [15], in 5 patients the NOGGO GIS V1 assay [16] and one patient had *BRCA1* class 5 mutation according to the Oncomine BRCA Research Assay from ThermoFisher Scientific. For 60 patients IHC AHRH and for 62 patients IHC SFRP2 staining was informative.

Clinical data was obtained from the Tumour Bank Ovarian Cancer Network ([www.toc-network.de](http://www.toc-network.de)) or the Charité Comprehensive Cancer

Centre (<https://cccc.charite.de>). The conduct of this study was approved by the local ethics committee (EA1/051/18 and EA1/110/22). Clinicopathological parameters of the patient cohorts are summarised in Supplementary Table 1.

### Targeted RNA sequencing

Forty-eight paired formalin-fixed, paraffin-embedded (FFPE) tissue samples of primary and recurrent tumours of 24 patients from the PRI-REC-Cohort ( $n = 24/85$ ) were prepared for HTG EdgeSeq analysis (provided by HTG Molecular Inc., Tucson, Arizona, USA).

For this purpose, H&E-stained large-area sections of the specimens were analysed by light microscopy, and sites with optimal tumour content were marked by an experienced gynecopathologist (S.D.E.). Corresponding unstained slides were forwarded to HTG, where tissue was scraped off and used for further processing. Workflow information is available on the HTG Web page (<https://www.htgmolecular.com/systems/chemistry>). Briefly, this method combines RNA extraction-free chemistry, a quantitative Nuclease Protection Assay and a qPCR for library preparation. The HTG EdgeSeq Oncology Biomarker Panel was used to measure the gene expression levels (mRNA) of 2,549 genes associated with tumour biology (Supplementary Table 2). Normalised libraries were analysed by Next Generation Sequencing (Illumina NextSeq Sequencer). After applying the previously stated inclusion and exclusion criteria, five of the sample pairs had to be excluded because of non-matching histotype ( $n = 3$ ) or NACT ( $n = 2$ ). Finally, 19 pairs (screening cohort, Supplementary Fig. 1a) could be included in further analysis (Supplementary Table 1).

### Immunohistochemistry

Immunohistochemical staining was performed semi-automatically on TMAs using a DISCOVERY XT/ULTRA autostainer (Ventana Medical Systems, Inc., Tucson, Arizona, USA). The following antibodies were used at dilutions previously tested on normal tissue: AHRH (1:3000, Abcam, Ref. No. ab108518), COL5A2 (1:100, Sigma-Aldrich, Ref. No. SAB4500385), FABP4 (1:1500, Abcam, Ref. No. ab92501), HMGC52 (1:200, Abcam, Ref. No. ab137043), ITGA5 (1:600, Abcam, Ref. No. ab112183), SFRP2 (1:25, Abcam, ab92667), WNT9B (1:500, Abcam, Ref. No. ab151220). Positive and negative control tissues for antibody establishment were selected based on the manufacturer's instructions and the Human Protein Atlas [17] (Supplementary Table 3). Universal negative controls of all TMAs were generated by omitting the primary antibody. If samples showed positivity ( $H$ -score  $\geq 20$ , Supplementary Table 4), the affected samples were revised and excluded from all analyses. The stained TMAs were digitalised using the Panoramic Slide Scanner (3D Histech, Budapest, Hungary).

### Methylation analysis

For 16 randomly selected HGSOc samples from the survival cohort, for which IHC data for AHRH and SFRP2 were available, a genome-wide methylation analysis was performed as previously described [18]. Briefly, tumour areas were punched out from the FFPE block for DNA extraction. Semi-automated DNA extraction was performed according to the manufacturer's instructions (Maxwell RSC FFPE Plus DNA Purification Kit, Custom, Promega). DNA quantities were measured using Qubit HS DNA assay (Thermo Fisher Scientific). DNA restoration was performed using the Infinium HD FFPE DNA Restore Kit and methylation analysis was performed using the Illumina Infinium MethylationEPIC BeadChip. All methylation data pre-processing was conducted in R using various methods as implemented in the ChAMP package. Raw signals were loaded from the IDAT files using the minfi package [19, 20]. A number of CpG sites were filtered out: all SNP-related sites; multi-hit sites; and CpGs located on chromosomes X and Y. Lastly, the beta values of the remaining CpG sites were normalised using FunNorm [21] followed by BMIQ [22]. Next, we selected the normalised beta values for CpGs that passed the above filters and extracted from the annotated file provided by the Illumina the CpGs mapped to *AHRH* (138 CpGs) and *SFRP2* (41 CpGs) genes.

### Liquid chromatography-mass spectrometry (LC-MS)

LC-MS analysis of cell lines was performed with an EASYnLC-1200 system (Thermo Fisher Scientific) connected to a trapped ion mobility spectrometry quadrupole time-of-flight mass spectrometer (timsTOF Pro2, Bruker Daltonik) with a nano-electrospray ion source (CaptiveSpray, Bruker Daltonik). Peptides were loaded on a 20-cm home-packed HPLC column (75- $\mu$ m inner diameter packed with 1.9- $\mu$ m ReproSil-Pur C18-AQ silica beads, Dr. Maisch). Peptides were separated over a 60 min gradient from 2

to 60% (0.5 min to 4%, 31.5 min to 20%, 15 min to 30%, 3 min to 60%, followed by a wash in 90% for 2 min and decrease to 50% in 7 min) in buffer B (0.1% formic acid and 90% ACN in LC-MS grade water) at 250 nl min<sup>-1</sup>. Buffer A consisted of 0.1% formic acid in LC-MS grade water. A column oven was used to keep the column temperature constant at 40 °C. For dia-PASEF analysis, we used a dia-PASEF method with 16 diaPASEF scans separated into 2 ion mobility windows per scan covering a 400–1200 *m/z* range by 25 Th windows and an ion mobility range from 0.60 to 1.43 Vs cm<sup>-2</sup>. The MS was operated in high sensitivity mode, with an accumulation and ramp time at 100 ms, capillary voltage set to 1400 V and the collision energy as a linear ramp from 20 eV at 1/K0 = 0.6 Vs cm<sup>-2</sup> to 59 eV at 1/K0 = 1.6 Vs cm<sup>-2</sup>. MS raw file analysis was performed with DIA-NN [23] and described in detail in the supplementary methods.

### Statistical analysis

Statistical analysis was performed using IBM SPSS Statistics 26 (Armonk, NY, USA), R 3.5.2 (R Project for Statistical Computing, RRID:SCR\_001905) and GraphPad Prism 9.0. Figures were created in SPSS, GraphPad Prism 9.0 and Biorender (<https://app.biorender.com>).

The count data was processed using the HTG parsing tool and scale-normalised using the trimmed mean of *M*-values (edgeR, RRID:SCR\_012802). To perform a differential gene expression (DEG) analysis according to primary and recurrent disease, linear models with empirical Bayes moderation (LIMMA, RRID: SCR\_010943) were fitted using a paired model design. Adjustment for multiple testing was carried out using the Benjamini-Hochberg method.

Exploratory analysis of the IHC protein level was done independently. The correlation of markers with clinical or pathological parameters was performed using the Chi<sup>2</sup> or Fisher's exact test. For different levels between *H*-scores between tumour samples and for in vitro experiments we first assessed whether the data followed a normal distribution using the Shapiro-Wilk normality test and the *F*-test was employed for calculating variance between groups. Next, for paired samples, *p*-values were determined with a paired *t*-test if data were normally distributed, and the non-parametric Wilcoxon-signed rank test was used for values with a non-normal distribution. For unpaired samples, *p*-values were determined with an unpaired *t*-test if the data were normally distributed, while the Mann-Whitney test was applied for values with a non-normal distribution. Correlation analysis between parameters was performed using Pearson's *r* coefficient.

To determine the prognostic impact of the evaluated markers on patient survival, univariate Kaplan–Meier survival analysis (Log-rank test) and multivariate Cox regression analysis (age at diagnosis ( $\leq 60$  versus  $>60$ ), FIGO stage (FIGO I–II versus FIGO III–IV), residual tumour (R0 versus R1)) were performed. Overall survival (OS) was defined as the time from the day of pathologic diagnosis until the patient's death, regardless of the cause. Progression-free survival (PFS) was defined as the time from diagnosis to occurrence of clinical progression, or recurrence, as measured by imaging. Optimal cutoffs for these calculations were obtained using the Cutoff Finder ([https://molpathoheidelberg.shinyapps.io/CutoffFinder\\_v1/](https://molpathoheidelberg.shinyapps.io/CutoffFinder_v1/)) and estimated based on OS [24]. *p*-values  $< 0.05$  were considered statistically significant in two-sided testing. The statistical tests used for every figure were investigated to be appropriate and the data meet the assumptions of the tests.

### Other methods

Other methods are included in the Supplementary Information.

## RESULTS

### Targeted RNA sequencing reveals differentially expressed genes in primary and recurrent HGSOC

A complex pipeline was designed to discover genes with potential key roles in HGSOC recurrence, validate the expression of their proteins, and to discover predictive biomarkers (Fig. 1a). To assess genes and biological pathways that might be associated with the process of tumour recurrence in HGSOC, we analysed 38 matched samples of primary and recurrent tumours from the PRI-REC-Cohort ( $n = 19$ , screening cohort). We found 373 genes to be differentially expressed between primary and recurrent samples after adjustment for multiple tests. As the cutoff criteria, genes with adjusted  $p < 0.05$  and  $|\log_2FC| > 0.8$  were considered significantly differentially expressed and therefore applicable for further analysis (Fig. 1b). This approach resulted in 233 DEGs, of which 199 (85.4 %) were expressed higher in the primary tumours and 34 (14.6 %) showed higher expression in the recurrent samples (Supplementary Table 5).

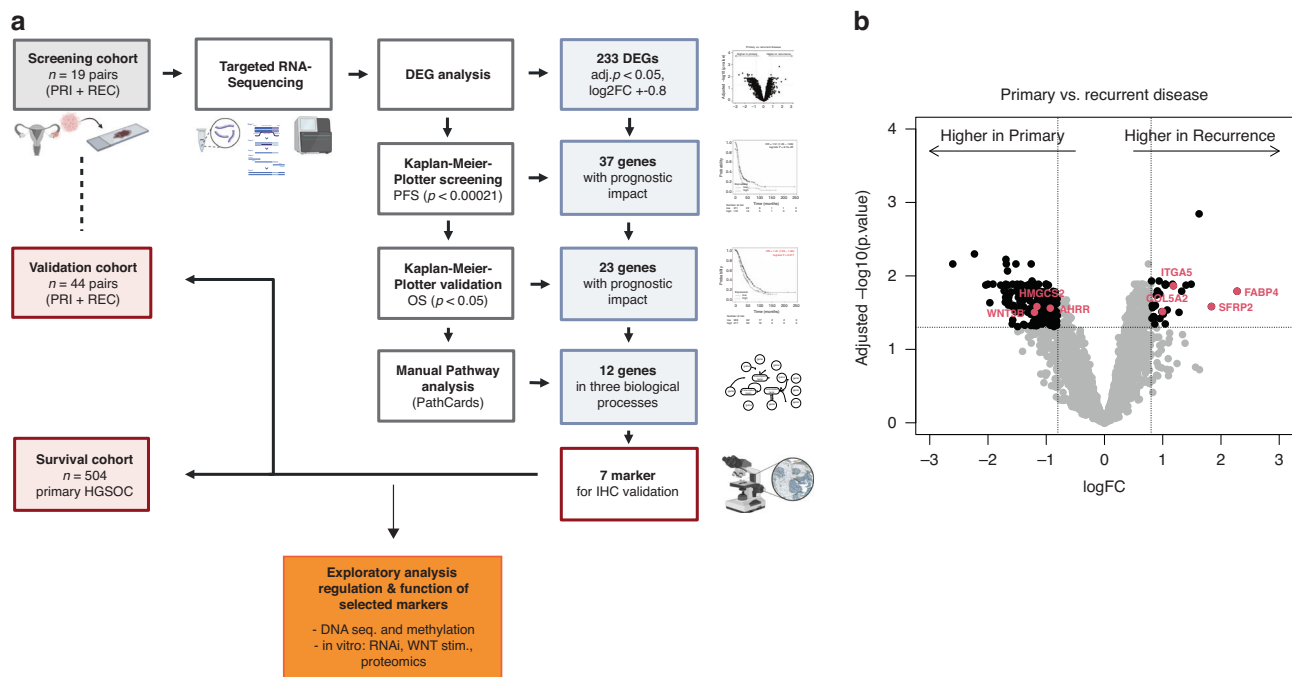


**Fig. 1 Biomarker selection procedure.** **a** Scheme of study design. Created with BioRender.com, **b** Volcano plot of differential gene expression analysis according to primary and recurrent disease. For each gene, the log fold-change ( $\log_2FC$ ) and the  $-\log_{10} p$ -value are plotted. The dotted lines indicate the set cutoff values for further analysis ( $p < 0.05$ ,  $|\log_2FC| > 0.8$ ). Red dots mark the seven markers chosen for IHC.

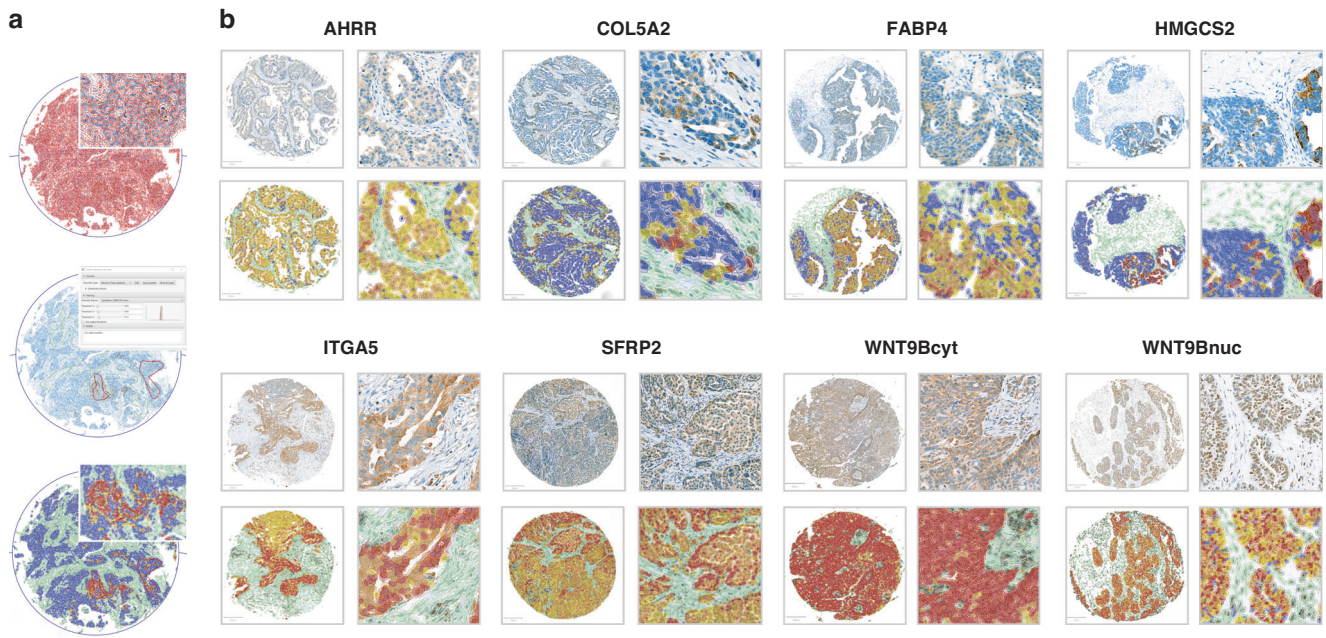


**Fig. 2 Immunohistochemical analysis.** **a** Workflow of digital image analysis using QuPath. **b** Representative IHC-staining, cell detection and classification. Detected cells were classified and colour-coded using QuPath. Blue, negative tumour cells. Yellow, weakly stained tumour cells. Orange, moderately stained tumour cells. Red, strongly stained tumour cells. Green, cells of the tumour-microenvironment with increasing darkness according to intensity of protein expression. Images on the right are magnifications of areas in the pictures on the left.

### In silico analysis identifies a prognostic impact for a subset of genes and indicates a key role of extracellular matrix organisation

To further test whether the identified DEGs are of clinical significance in primary OC, we conducted a Kaplan–Meier Plotter survival analysis [25] for all 233 DEGs individually (Supplementary Table 6). In this analysis, 37 genes were identified as predictors for PFS of serous OC patients on the mRNA level ( $p < 0.0002$ ; Bonferroni). Twenty-three of these 37 genes furthermore showed significant association with the OS ( $p < 0.05$ , Bonferroni, Supplementary Table 7). Twelve of these genes showed high expression in the primary tumour samples and 11 were upregulated in the recurrences (Supplementary Table 8).

To analyse which pathways might be affected by the DEGs in recurrent HGSOc, we performed gene ontology enrichment analysis. Analysis of the 11 genes upregulated in recurrent tumours with a significant prognostic impact, revealed enrichment of biological processes associated with collagen fibril organisation (GO:0030199), extracellular matrix organisation (GO:0030198) and supramolecular fibre organisation (GO:0097435). The same analysis of the 12 genes, that showed an upregulation in the primary tumours, did not lead to significant results.

To nail down genes most suitable for further analysis via IHC on tissue samples, we determined the biological function of all 23 DEGs via Pathcards.

This analysis revealed that 12 of the prognostic DEGs were clustering into three major biological functional groups which can be summarised as “Extracellular matrix organisation”, “Regulation of lipid metabolism by Peroxisome proliferator-activated receptor alpha (PPARalpha)” and “WNT signalling” (Supplementary Table 8). In conjunction of earlier studies [7] by our consortium and extensive literature review we focused on 7 genes. Three of these seven genes (*AHRR*, *HMGCS2*, and *WNT9B*) showed a higher expression in the primary tumours and have not been evaluated or described before in this context. Four genes (*FABP4*, *SFRP2*, *ITGA5*, and *COL5A2*) had an increased expression level in the recurrent tumours and were chosen as representatives for the above-mentioned pathways (Supplementary Figs. 2a–g and 3a–g).

### Compartment-dependent expression patterns in tumour samples of HGSOc

To analyse the protein expression of these seven genes we used a specific pipeline employing digital pathological analysis of the IHC-stained TMA slides using QuPath (Fig. 2a). Antibody staining was detected in both primary and recurrent tumours and was mainly located in the cytoplasmic cell compartment with only *WNT9B* showing additional nuclear and *ITGA5* showing sporadic membranous staining (Fig. 2b).

In addition to the detection in the tumoral compartment, the proteins were furthermore found in specific cells of the TME (Supplementary Fig. 4a–h). For example, *FABP4* showed high expression in tumour surrounding adipocytes and *COL5A2* was expressed in tumour-associated fibroblasts. While the expression of *HMGCS2* was very clear in tumour cells, it was predominantly negative in the stroma (Supplementary Fig. 4d). Low *H*-scores determined by QuPath proved to be artificial after reviewing by a pathologist (E.T.T), hence the stromal expression of *HMGCS2* was not included in the further analyses.

Protein expression distributions in the primary tumours (PRI-Cohort) showed a negative median *H*-score (0–1) for *HMGCS2* (0.04) and low median *H*-scores (1–100) for *FABP4*, *COL5A2*, *AHRR*, cytoplasmatic *WNT9B* and *ITGA5* (3.94; 7.2; 34.15; 80.81; 93.56) in the tumour compartment. Nuclear *WNT9B* expression (median *H*-score: 105.17) was moderate (*H*-score: 101–200) and median *SFRP2* expression (*H*-score: 234.56) was strong (*H*-score: 201–300) (Supplementary Fig. 4a–h).

### *AHRR* and *SFRP2* are differentially expressed in primary and recurrent tumour samples

Next, we aimed to validate differences in gene expression between recurrent versus primary tumours on the protein level. Therefore, we analysed tumour compartments in which our gene set was differentially expressed, hence moving our study from a bulk level to a cellular level (Fig. 3a, b).

The median *AHRR* protein expression in the tumour cells in primary samples was 104.15 (*H*-score, range: 0.28–212.13, Supplementary Table 9) but 13.43 (*H*-score, range: 0–182.92) in

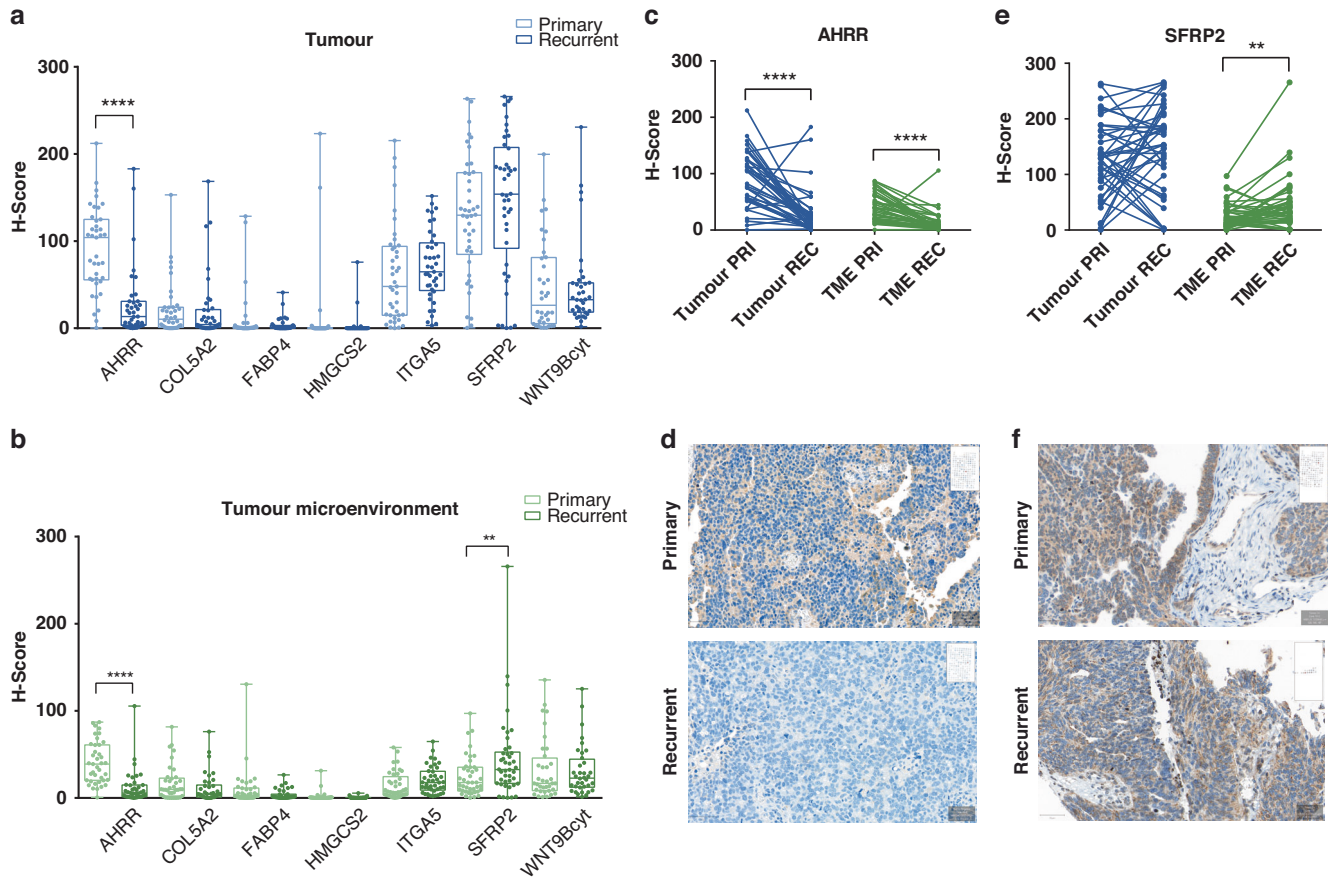


**Fig. 3 Differential expression on the protein level.** **a** Boxplots of differential expression in the tumour compartment of primary (PRI) and recurrent (REC) samples, **b** Differential expression in the tumour microenvironment (TME). The 25–75th percentile of expression is represented by the boxes and the whiskers show minimum and maximum. Circles on the whiskers represent individual data points. Light colouring indicates the expression in primary samples, dark colouring for recurrent samples. **c** Before and After Plot of AHRR *H*-scores in the paired primary and recurrent HGSOc from the validation cohort ( $n = 39$ ). **d** Example for AHRR protein expression in a primary and a recurrent sample, scale bars: 50  $\mu\text{m}$ . **e** Distribution of SFRP2 *H*-scores in the paired primary and recurrent samples ( $n = 42$ ). **f** Example for SFRP2 staining in a primary sample and a recurrence. Scale bars: 50  $\mu\text{m}$ . Significance levels were determined using the Wilcoxon-signed rank test (\*\* $p < 0.01$ , \*\*\*\* $p < 0.0001$ ).

the recurrences, showing a significantly higher AHRR expression in the tumour cells within the primary HGSOc group ( $n = 39$  pairs, Wilcoxon  $p < 0.0001$ , Fig. 3c, d). Additionally, AHRR was higher expressed in the TME of primary samples when compared to the TME of recurrent samples ( $n = 39$  pairs, Wilcoxon  $p < 0.0001$ , Fig. 3c).

The contrary observation was made for SFRP2 (Fig. 3e, f), showing a higher median expression in the cells of recurrent tumour samples (32.59 *H*-score, range: 0.39–265.72) when compared to the matched primary ones (17.71 *H*-score, range: 0.23–97.06). This difference was statistically significant ( $n = 42$  pairs, Wilcoxon  $p = 0.009$ ) but restricted to the TME. In pairwise testing, median *H*-scores of the tumour compartment did not show expression differences for SFRP2 ( $n = 42$  pairs, Wilcoxon  $p = 0.365$ ). Interestingly, none of the other differentially expressed genes showed significant differences in the matched pairs at the protein level (Fig. 3a, b).

#### Protein expression of FABP4, SFRP2 and cytoplasmic WNT9B correlate with clinical and histological parameters

The associations between the expression levels of the seven IHC markers and clinicopathological parameters including age, FIGO stage, regional lymph node involvement (pN) and residual tumour (R) were analysed in the survival cohort. FABP4 protein expression in the tumour cells and the presence of regional lymph node

metastases were inversely associated ( $\chi^2 = 5.309$ ,  $p = 0.021$ ). N1 status was more common in patients with low FABP4 values.

Additionally, high expression of cytoplasmic ( $p = 0.049$ ) and nuclear ( $p = 0.043$ ) WNT9B in the TME was found in older patients (age at diagnosis  $> 60$  years) (Supplementary Table 10).

#### Expression of AHRR and SFRP2 has a prognostic impact on HGSOc

The survival analysis was performed on primary tumours, using IHC data from the tumour compartment and the TME independently. Information on OS was available for all 504 patients and PFS data was available for 329 patients (65.3%). Median follow-up was 85.8 months (95% CI 70.1–101.5 months) in the survival cohort. As no cutoff values were primarily established for our markers, we defined them with the Cutoff Finder [24] as described in supplementary materials and methods (Supplementary Table 11).

For AHRR expression in the tumour cells, IHC data was available for 476 patients and the optimal prognostic cutoff out of 209/449 (46%) possible cutoffs was 55.16 (*H*-score). 325 patients (68.3%) showed a protein expression below this cutoff and 151 (31.7%) showed a protein expression above it. Median OS in the low expressing group was 37.4 months (95% CI 33.3–41.4 months) as opposed to 71.0 months (95% CI 58.2–83.9) for the high-expressing group ( $p < 0.001$ ; Supplementary Table 11 and Fig. 4a).

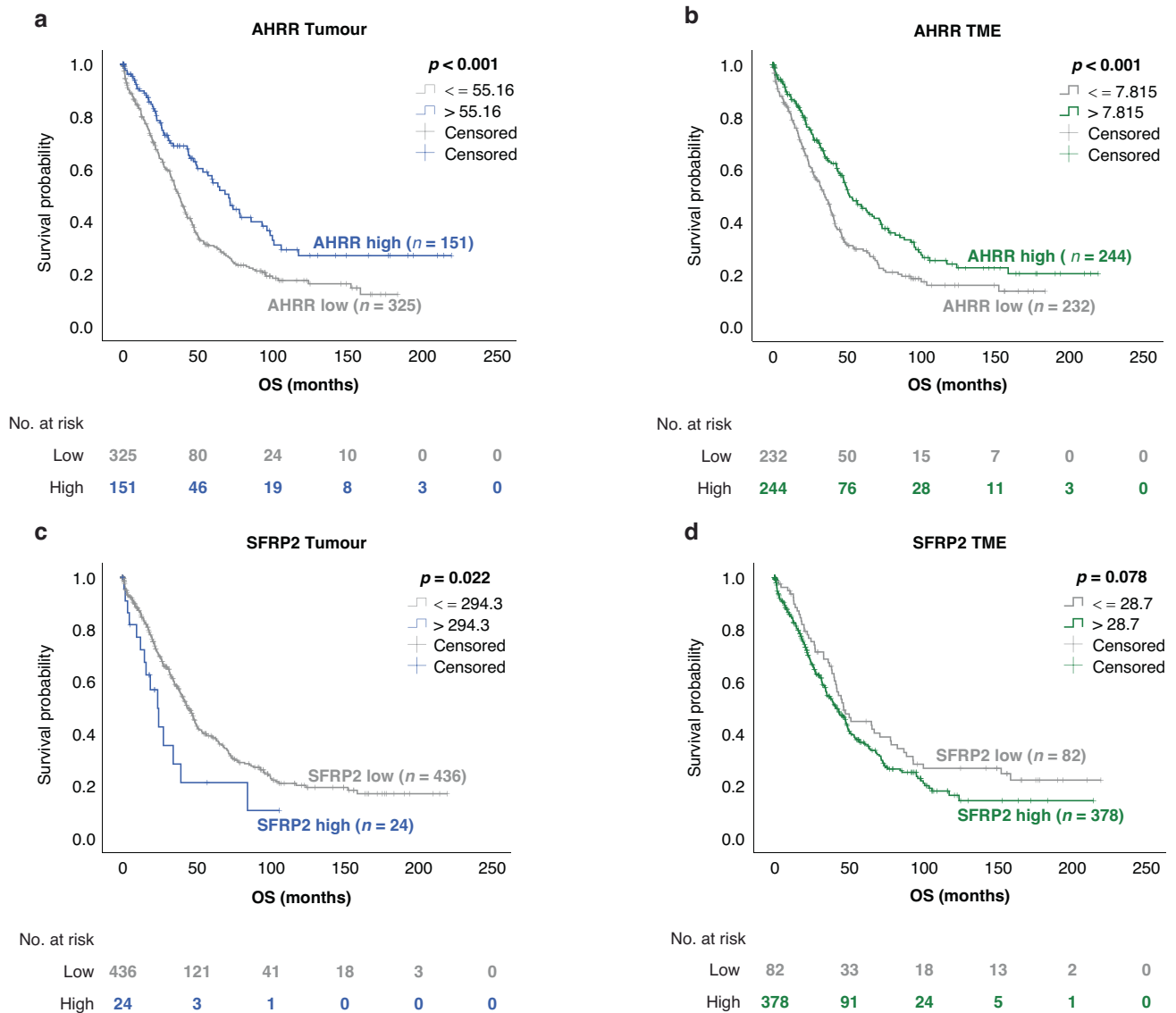


**Fig. 4** Kaplan–Meier survival curves according to the protein expression of AHRR and SFRP2 in the survival cohort. Cohorts were dichotomised by optimal  $H$ -score cutoffs. **a, b** OS according to AHRR expression in the tumour and the tumour-microenvironment (TME). **c, d** OS according to SFRP2 expression in the tumour and the TME. Significance levels were determined using the log-rank test.

When splitting the entire cohort according to the AHRR expression in the TME (cutoff: 7.815), a significantly superior OS within the high-expressing group was observed. In this group ( $n = 244$ , 51.3%) median OS was 52.0 months (95% CI 41.2–62.7 months) while in contrast a median OS time of 35.2 months (95% CI 29.8–40.5 months) was seen in the group with low ( $n = 232$ , 48.7%) AHRR expression ( $p < 0.001$ , Fig. 4b). This positive prognostic impact also remained significant regarding the OS in the multivariate analysis for both tumour (HR 0.56, 95% CI 0.4–0.78,  $p = 0.001$ ) and TME (HR 0.62, 95% CI 0.47–0.81,  $p < 0.001$ ), verifying that AHRR is an independent prognostic marker in HGSO, regardless of the compartment (Table 1).

Differences in PFS time according to tumoral AHRR expression were non-significant ( $p = 0.095$ , Supplementary Fig. 5a). The analysis of a correlation of stromal AHRR expression and PFS verified the OS results with a median PFS of 17.6 months (95% CI 15.2–20.1) for the AHRR low group and 22.6 months (95% CI 18.5–26.8) for the AHRR high group ( $p = 0.041$ , Supplementary Fig. 5b). Again, the prognostic value for PFS could be confirmed in

the multivariate analysis (HR 0.72, 95% CI 0.55–0.96,  $p = 0.024$ , Supplementary Table 11).

A significant correlation with patient survival was also found for SFRP2, showing a lower median OS (23.8 months, 95% CI 14.7–32.9 months) for patients with a high expression of SFRP2 in their tumour cells (cutoff: 294.3;  $n = 24/460$ , 5.2%) as compared to the median OS time (44.0 months, 95% CI 39.1–48.9 months) for patients with a low expression ( $n = 436$ , 94.8%). This finding was statistically significant for the OS when SFRP2 expression in tumour cells was considered ( $p = 0.022$ , Fig. 4c), but not for expression in the TME ( $p = 0.078$ , Fig. 4d) or when PFS was considered for SFRP2 expression in tumour cells ( $p = 0.061$ , Supplementary Fig. 5c) or TME ( $p = 0.566$ , Supplementary Fig. 5d). Although the cutoff of 294.3 was only one out of 0.9% significant cutoffs found by the Cutoff Finder, its significance was retained in the multivariate analysis for the OS, indicating the independent negative prognostic impact of SFRP2 (HR 2.6, 95% CI 1.5–4.4,  $p = 0.001$ , Table 1). As SFRP2 acts as a regulator of the Wnt-signalling pathway and tumoral SFRP2 and stromal WNT9B showed an inverse impact on patient survival (Supplementary

**Table 1.** Multivariate Cox regression model for overall survival in the survival cohort with regard to AHRR and SFRP2 expression in the tumour cells and the TME.

AHRR	Tumour			TME		
	OS (n = 334)			OS (n = 334)		
Variable	HR	95% CI	p	HR	95% CI	p
Age > 60	1.23	0.943–1.603	0.128	1.29	0.989–1.683	0.060
FIGO > II	2.68	1.187–6.067	<b>0.018</b>	2.59	1.146–5.870	<b>0.022</b>
Residual tumour	2.01	1.526–2.639	<b>&lt;0.001</b>	2.01	1.527–2.639	<b>&lt;0.001</b>
AHRR high	0.56	0.403–0.776	<b>0.001</b>	0.62	0.469–0.805	<b>&lt;0.001</b>
SFRP2						
OS (n = 316)						
Variable	HR	95% CI	p			
Age > 60	1.23	0.937–1.620	0.136			
FIGO > II	2.40	1.059–5.420	<b>0.036</b>			
Residual tumour	2.11	1.593–2.799	<b>&lt;0.001</b>			
SFRP2 high	2.57	2.566–1.499	<b>0.001</b>			

TME tumour microenvironment, OS overall survival, n number of patients, HR hazard ratio, CI confidence interval, FIGO Fédération Internationale de Gynécologie et d'Obstétrique. Bold values indicate statistical significance  $p < 0.05$ .

Table S11), we tested whether a combination of these two markers would be of further relevance. This analysis was performed for SFRP2 and cytoplasmatic WNT9B only, as data on WNT9Bnuc combinations were limited. Patients with SFRP2 + / WNT9Bcyt- status ( $n = 4$ ) were found to have the worst OS when compared to the other three combinations, while patients with SFRP2-/WNT9Bcyt+ status ( $n = 128$ ) had the longest survival interval ( $p = 0.035$ ). The same observation could be made for the PFS, where survival was significantly better for patients with SFRP2-/WNT9Bcyt+ status ( $p = 0.021$ , Supplementary Fig. 6a, b).

In contrast to AHRR and SFRP2 other markers did not maintain significance in multivariate analysis (Supplementary Tab. 11) or could not be confirmed as being differentially expressed between primary and recurrent tumours on the protein level. COL5A2, HMGS2 and ITGA5 expressed in the tumour compartment and cytoplasmatic as well as WNT9Bnuc in the stroma were favourable prognostic factors for OS ( $p < 0.05$ , Supplementary Fig. S7a–k) in univariate analysis. In multivariate analysis this significant correlation could be obtained only for stromal WNT9Bcyt (HR 0.64, 95% CI 0.47–0.88,  $p = 0.005$ ) and WNT9Bnuc (HR 0.39, 95% CI 0.17–0.9,  $p = 0.028$ ). For PFS cytoplasmatic WNT9B was found to be associated with better patient survival in the tumour cells ( $p = 0.029$ ) as well as in the stroma ( $p = 0.017$ ), which was confirmed (HR 0.67, 95% CI 0.48–0.92,  $p = 0.014$ ) by multivariate analysis for the expression in the TME (Supplementary Fig. 8a–k and Supplementary Table 11). Interestingly, stromal FABP4 was revealed to correlate with a worse PFS ( $p = 0.043$ , Supplementary Fig. 8d, multivariate analysis: HR 1.41, 95% CI 1.06–1.86,  $p = 0.017$ ).

Additionally, we wanted to check if the HRD status has any impact on the protein expression of AHRR and SFRP2. For this purpose, we used a third cohort for which HRD status was available. No association was detected between the HRD status and AHRR  $H$ -scores in tumour ( $p = 0.52$ , Supplementary Fig. 9a) or stroma cells ( $p = 0.7$ , Supplementary Fig. 9b) and SFRP2  $H$ -score in tumour ( $p = 0.72$ , Supplementary Fig. 9c) or stroma cells ( $p = 0.87$ , Supplementary Fig. 9d).

### Exploratory analysis of the regulation and function of AHRR and SFRP2 in HGSOc

We wanted to understand the mechanism responsible for the dysregulated protein expression of AHRR and SFRP2 in HGSOc. First, we analysed DNA sequence alterations including mutations and copy number changes affecting these two genes in HGSOc

samples from TCGA [9]. Out of 273 tumours analysed, 26 (9.5%) exhibited mutations or amplifications in AHRR, while 7 (3%) displayed copy number changes (amplifications and deletions) in SFRP2 (Supplementary Fig. 10a). We also performed a comparative assessment of the prevalence of AHRR and SFRP2 genomic sequence alterations between long-term and short-term survivors, but no significant differences were observed (Supplementary Fig. 10b). Second, we assessed the DNA-methylation profiles of both genes and performed genome-wide methylation profiling in 16 patients with HGSOc for which we had analysed AHRR and SFRP2 protein levels. We observed a synchronised hypermethylation of most of the 138 CpGs associated with AHRR, with an average methylation level of 0.67 (max. 1) (Fig. 5a and Supplementary Table 12). For SFRP2, which is overexpressed in HGSOc, we observed a synchronised hypomethylation of the 41 CpGs associated with this gene, with an average methylation level of 0.36 (Fig. 5b and Supplementary Table 13). Upon correlating the  $H$ -scores of AHRR and SFRP2 and methylation levels of the matching CpGs, we observed that 15 CpGs associated with AHRR (4 located in regulatory CpGs intragenic regions—body island) showed a significant negative correlation between their methylation and the protein levels (Supplementary Fig. 10c); and five CpGs associated with SFRP2 (4 located in the transcription start site—TSS) showed a significant negative correlation between methylation and the protein levels (Supplementary Fig. 10d). Hence, it seems that the two genes are potentially dysregulated in HGSOc by aberrant focal DNA methylation.

To explore the function role of AHRR and SFRP2 protein expression in HGSOc, we tested their impact on cell proliferation using the DepMap Database. We observed that the knock-out of these genes compared to PAX8 (an established tumorigenic factor in HGSOc) [26] has no influence on tumour cell proliferation in 57 different epithelial ovarian cancer cell lines (Supplementary Fig. 11a). We analysed the basal expression of AHRR in five TP53 mutated ovarian epithelial tumour cell lines and observed that AHRR has the highest expression in the EFO21 cell line (isolated from malignant ascites) (Supplementary Fig. 11b). Therefore, we selected this cell line for subsequent analysis to investigate the global proteome differences after AHRR knockdown (KD), using two different siRNAs (Supplementary Fig. 11c). Global proteome profiling by LC-MS analysis resulted in ~7,000 quantified proteins per single measurement and over 8000 proteins in total (Supplementary Fig. 11d and Supplementary Table 14). Albeit

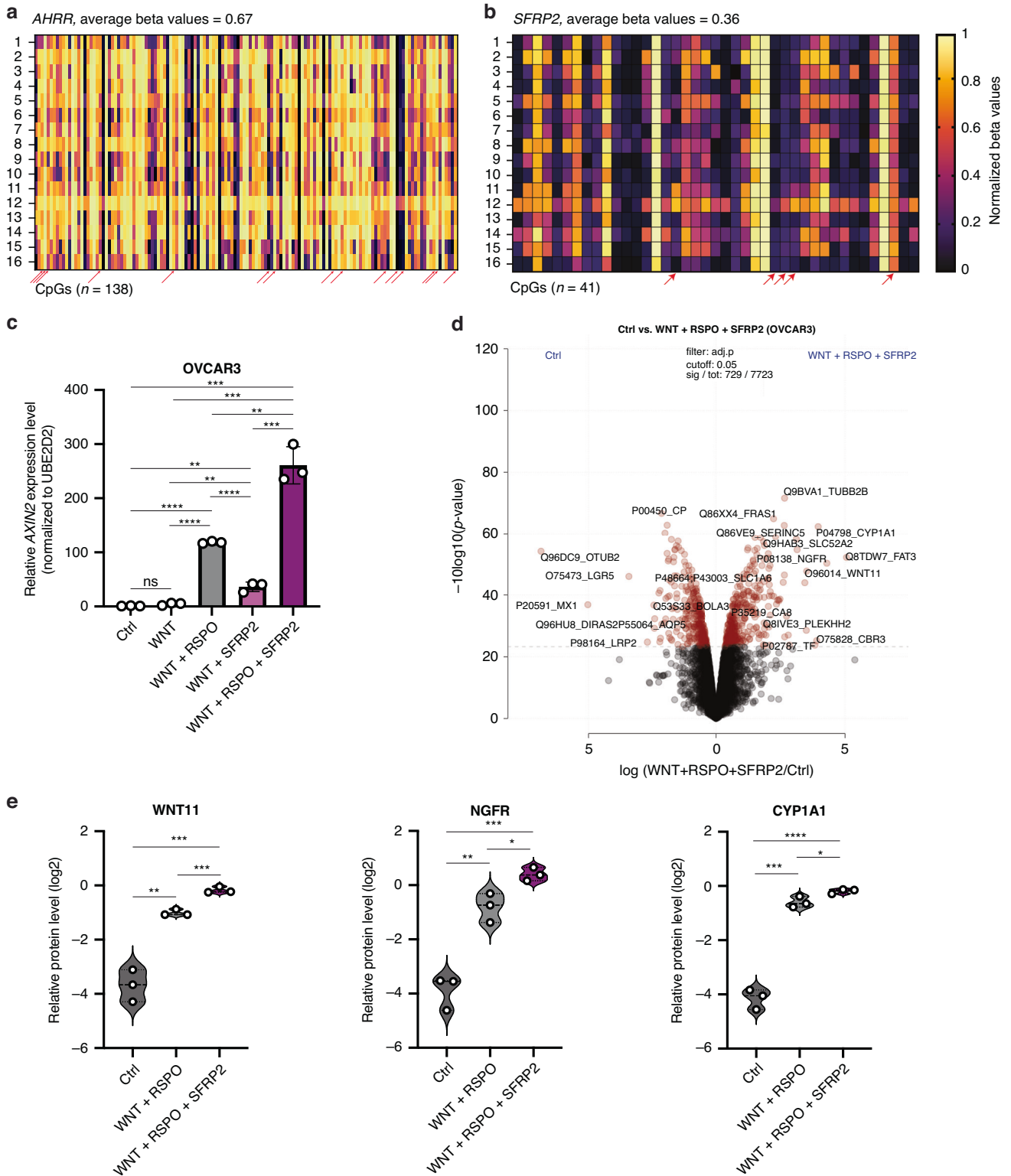


**Fig. 5 Exploratory analysis of the regulation and function of AHRR and SFRP2 in HGSOc.** **a** Methylation levels (normalised beta values) in 138 CpGs associated with *AHRR* and **b** in 41 CpGs associated with *SFRP2* in 16 patients with HGSOc for which also the protein expression of the two genes was available. With red arrows are marked the CpGs that negatively correlated with the *H*-score of the matching protein. **c** *AXIN2* mRNA level in OVCAR3 cells without treatment (Ctrl), and with WNT, WNT + RSPO, WNT + SFRP2 and WNT + RSPO + SFRP2. **d** Volcano plot of the pairwise proteomic comparison between the OVCAR3 control and OVCAR3 WNT + RSPO + SFRP2 stimulated cells. Significantly expressed proteins are highlighted in red (moderated two-sided *t*-test, FDR < 0.05). For both groups, the experiment was done in biological triplicates. **e** Relative protein level of WNT11, NGFR, and CYP1A1 in Control versus WNT + RSPO stimulated versus WNT + RSPO + SFRP2 stimulated OVCAR3 cell lines. Significance levels were determined using the unpaired *t*-test (ns = not significant, \**p* < 0.05, \*\**p* < 0.01, \*\*\**p* < 0.001, \*\*\*\**p* < 0.0001).

protein fold changes only revealed small differences, with one protein significantly upregulated (adj.  $p$ -value < 0.05) in the AHRR KD, the transcriptional regulator MLXIP (Supplementary Fig. 11e), pathway enrichment analysis based on the protein fold-change between AHRR KD versus control cells resulted in higher levels of proteins related to epithelial-to-mesenchymal transitions in AHRR KD cells, such as integrin cell surface, collagen degradation, collagen formation, degradation of the extracellular matrix and extracellular matrix organisation (Supplementary Fig. 11f). This finding is in line with reports showing that low levels of AHRR are involved in invasion and migration in vitro and metastases in vivo in multiple cancers [27]. Collectively, the data support a potential tumour-suppressive role of AHRR, in strong agreement with our clinical samples data.

SFRP2 is a secreted modulator of WNT signalling [28] and was initially understood as a negative regulator of WNT signalling due to its ability to restrict the binding of Wnt ligands to their receptor [29]. More recent data show that SFRP2 can act as a negative or positive factor of WNT signalling, depending on the context [30]. Yet, its role in ovarian cancer is not defined. To functionally investigate the role of SFRP2 in ovarian cancer, we cultivated five epithelial ovarian cancer cell lines in the absence and presence of extracellular WNT effectors, including WNT3 (WNT) alone; WNT and RSPO1 (RSPO); WNT and SFRP2 (recombinant human protein); and WNT, RSPO and SFRP2 and tested the level of *AXIN2* as a WNT/ $\beta$ -catenin target gene [31]. We found that all cell lines were WNT-responsive, as the addition of WNT and the co-ligand RSPO to the medium-activated *AXIN2*. In all five cell lines, SFRP2 had no significant inhibitory effect on WNT signalling, and in OVCAR3 cells (isolated from malignant ascites) SFRP2 significantly further activated *AXIN2* compared to the activation provided by WNT plus RSPO (Fig. 5c and Supplementary Fig. 11g), suggesting a role of SFRP2 as a WNT activator in a subset of ovarian cancers. Next, we performed MS-based proteomic profiling to study the global effects of WNT activation and the consequence of SFRP2 addition. Our analysis resulted in ~7500 quantified proteins per single replicate (Supplementary Fig. 11h and Supplementary Table 15). By comparing OVCAR3 control to OVCAR3 with WNT + RSPO + SFRP2, we observed pronounced global protein level changes with indications of WNT signalling activation, with significant overexpression of WNT11 (Fig. 5d), a non-canonical WNT signalling molecule with a role in cancer [32]. Among the most upregulated proteins with SFRP2 addition, besides WNT11, were nerve growth factor and its receptor (NGFR) and CYP1A1 which showed a more significant upregulation in WNT + RSPO + SFRP2 versus control or WNT + RSPO (Fig. 5e). Previous studies have shown that NGFR is linked to WNT/ $\beta$ -catenin signalling and activates ovarian cancer tumour spread [33], while CYP1A1 was shown to be overexpressed in ovarian cancer clinical samples and to play a carcinogenic role [34]. Taken together, our functional investigations further support a tumour-suppressive role of AHRR and an oncogenic function of SFRP2 in ovarian epithelial cancer.

## DISCUSSION

In the present study, we interrogated information on DEGs in primary and recurrent HGSOC in the quest for clinically applicable biomarkers. Targeted RNA sequencing and in silico survival analysis revealed a prognostic impact of 23 genes. Further IHC analysis of seven markers (AHRR, COL5A2, FABP4, HMGCS2, ITGA5, SFRP2 and WNT9B) demonstrated significant differences for AHRR being lower and SFRP2 being higher expressed in recurrent HGSOC. To test if these markers could serve as prognostic biomarkers already in primary tumours survival analysis was performed in a large cohort of 504 patients with primary HGSOC and demonstrated a favourable prognostic significance of high AHRR and low SFRP2 expression. In vitro data further

supported the tumour suppressor role of AHRR and the pro-tumorigenic role of SFRP2.

Previous studies have shown that the modulation of the extracellular matrix and the tumour immune microenvironment are important mechanisms by which ovarian cancer cells might regulate tumour progression in recurrent or metastatic OC [6, 11, 12, 35]. Kreuzinger et al. defined primary and recurrent HGSOC samples as immune active or immune silent based on an unsupervised clustering method following RNA sequencing. Immune active recurrent samples showed an upregulation of genes involved in the remodelling of the extracellular matrix (e.g., *POST*, *COMP*, *COL5A2*) or genes like *SFRP2* and *ADH1B*. Primary samples with an immune active status additionally overexpressed genes associated with adipose tissue remodelling (e.g., *FABP4*, *GPD1*, *PLIN1*) [7]. Further studies on the immune modulation [6, 11, 12, 35] and angiogenesis [13] in primary and recurrent OC were based on the evaluation of specific IHC markers such as MVD, VEGF-A, MHC1, MHC2, PD-L1, IDO or different lymphocyte markers and showed increased expression of CD4+, MHC1 [12], PD-L1 [6, 35] and IDO [6], as well as higher levels of regulatory T cells [11] in recurrent samples.

In our study, we took a novel approach. It comprises an analysis of DEGs in primary and recurrent HGSOC and complements the aforementioned studies by adding a biomarker selection procedure based on in silico survival analysis and evaluation on a large cohort of primary tumours. During this process, we identified AHRR and SFRP2 as being consistently differentially expressed and with a significant prognostic potential for predicting OS.

The repressor of the aryl-hydrocarbon receptor (AHRR) showed an expression profile in line with the current understanding of it as a tumour suppressor [36] being higher expressed in primary tumours versus relapse. Patients with high AHRR expression displayed a significant increase in OS.

AHRR negatively regulates AHR signalling by competing with the AHR complex for its interaction with the aryl-hydrocarbon receptor nuclear translocator, thereby suppressing AHR signalling [37]. AHR is consistently active in a variety of human cancers and has several oncogenic functions [38], among them the mediation of pro-tumorigenic immunosuppression [39] and epithelial-mesenchymal transition [40]. AHR also dysregulates BRCA1 [41] expression, a crucial tumour suppressor in HGSOC and is additionally correlated with an unfavourable prognosis in OC [42]. Nevertheless, we could not detect an association of protein expression of AHRR with HRD status. Interestingly, AHR signalling was recently found to be the highest-ranking dysfunctional pathway in FIGO stage IV serous OC [43]. Therefore, regulation of AHR activation via AHRR expression might indicate an important anti-oncogenic mechanism in primary tumours [44]. In favour of this hypothesis there are recent observations in breast cancer showing that high *AHRR* mRNA levels are associated with favourable metastasis-free survival [45]. On the contrary, loss or downregulation of AHRR is proposed to have pro-oncogenic functions and drives tumour progression. To strengthen this hypothesis, we performed additional exploratory studies regarding the mechanism of AHRR downregulation and downstream function in OC. Genome-wide methylation analysis showed *AHRR* hypermethylation in HGSOC, and 15 CpGs showed an inverse correlation with matched protein expression. These 15 CpGs are located in the gene body, and four of them in intragenic CpG islands. Hypermethylation of gene-body CpGs can induce activation of transcription, yet the role of intragenic CpG islands is more complex and not fully understood. These regions, if hypermethylated can also inhibit gene transcription and have functions similar to promotor or enhancer regions [46]. Downstream analysis of AHRR function showed no impact on cell proliferation, rather proteomic studies revealed upregulation of proteins associated with epithelial-mesenchymal transition following AHRR KD. This observation is in line with previously published data showing that

low AHRR levels in different cancers could induce resistance to apoptosis and increases the migratory potential of tumour cells [27, 36].

*SFRP2*, the secreted frizzled-related protein 2, encodes an extracellular Wnt-signalling modulator, which directly interacts with Wnt proteins. *SFRP2* can act as a Wnt-suppressing or -activating factor in different tissue contexts and, therefore, exert tumour-suppressive or -promoting roles. Wnt-activating and tumour-promoting roles of *SFRP2* have previously been identified in colon and lung cancer, as well as in glioblastoma [47–49], and our study suggests a similar role in ovarian cancer. In five ovarian cancer cell lines, *SFRP2* did not inhibit WNT signalling and more interestingly, in one cell line, *SFRP2* activated WNT signalling. We confirmed this activation by performing MS spectrometry, observing the upregulation of WNT11, a member of the non-canonical WNT signalling pathway. Furthermore, we observed an upregulation upon *SFRP2* stimulation of other proteins with oncogenic function in HGSOc such as NGFR and CYP1A1, suggesting a potentially more complex tumorigenic function of *SFRP2* in HGSOc.

Our IHC analysis also points to a pro-tumorigenic function of *SFRP2*. *SFRP2* expression was higher in the stromal compartment of the recurrences and furthermore correlated with worse survival. These findings are in line with a study from Mariani et al. [50] where *SFRP2* was found to be overexpressed in OC bowel metastases when compared to primary samples. In comparison to our study, they could only show the differential expression on the RNA level, but also described the association of high *SFRP2* RNA expression with poor overall survival in a HGSOc patient cohort [50]. *SFRP2* gene expression was furthermore significantly upregulated in HGSOc specimens following NACT [51, 52] and Yuan et al. report *SFRP2* as part of a cluster consisting of nine key genes, able to predict high-risk patients with worse survival probability [53]. These results suggest a potential role of *SFRP2* as a biomarker for poor survival.

Mechanisms of *SFRP2* overexpression are not yet clear as the findings of several previous studies indicate a downregulation of *SFRP2* in OC due to methylation of its promoter region [54–56] and *SFRP2*'s potential to inhibit migration of OC cells [57]. In order to clarify the mechanism of *SFRP2* regulation in HGSOc, we performed genome-wide DNA-methylation analysis of patient samples. Our data revealed that *SFRP2* is hypomethylated in HGSOc and 4 CpGs located in the TSS showed a negative correlation to the matching protein *H*-score.

For *SFRP2* our protein-based analysis is consistent with the results obtained by using the Kaplan–Meier-Plotter on mRNA levels. Surprisingly, high AHRR expression indicated increased OS in our own study, but the opposite direction was predicted by in silico survival analysis. The mRNA-based Kaplan–Meier analysis is furthermore puzzling since AHRR expression consistently indicated a tumour suppressor function in our own RNA and protein analysis in the PRI-REC cohort. Regarding prognosis, congruent results were obtained from our survival analysis of patients with primary HGSOc. These differences might be explainable by the fact that *TP53* mutation status was not available for all patients diagnosed with serous tumours in the datasets included in the Kaplan–Meier-Plotter [25], which is why the in silico analysis also included a small number of low-grade serous tumours. Additional differences might be caused by the circumstance that microarray gene expression data is obtained from the bulk analysis, which leads to the admixture of signals from the tumour and the stromal compartments [58].

The small sample size of our PRI/REC cohort and of our validation cohort could lead to data overfitting. We would like to point out that paired primary and relapse samples are difficult to obtain and we conducted our analysis with the best available sample size. Furthermore, we reduced the risk of overfitting the data by using conventional statistical methods as opposed to

machine learning approaches and by confirming our findings in independent cohorts and by different methods. We used a highly standardised method for digital image analysis, which allows the separate analysis of the tumour and the TME, possibly leading to more precise results. Nevertheless, IHC analysis has some biases too, e.g., tissue processing or antibody specificity. To clarify the question on the correlation of mRNA and protein in our survival cohort, RNA sequencing data would have been needed ideally combined with tissue from relapse which is a limitation of our study. As we used optimised cutoffs for survival analysis, additive prospective clinical research needs to validate the prognostic implication of the markers on the survival of HGSOc patients.

As a conclusion, we present a highly explorative analysis of the differences in RNA and protein expression between primary and recurrent HGSOc, which lays the foundation for further research. Our results show that AHRR (tumour suppressor) and *SFRP2* (oncogene) are differentially expressed between primary and recurrent tumours both on the gene and the protein level and furthermore act as protein-based prognostic markers for HGSOc. Overall, the present study provides novel insights into the potential biological pathways and protein signatures involved in the process of recurrence and poor survival in HGSOc, *en passant* coming up with two potential prognostic biomarkers for advanced HGSOc.

#### DATA AVAILABILITY

The datasets used during this study are available from the corresponding author upon reasonable request.

#### REFERENCES

- Siegel RL, Miller KD, Fuchs HE, Jemal A. Cancer Statistics, 2021. *CA Cancer J Clin.* 2021;71:7–33.
- Lheureux S, Gourley C, Vergote I, Oza AM. Epithelial ovarian cancer. *Lancet.* 2019;393:1240–53.
- Torre LA, Trabert B, DeSantis CE, Miller KD, Samimi G, Runowicz CD, et al. Ovarian cancer statistics, 2018. *CA Cancer J Clin.* 2018;68:284–96.
- Berek JS, Renz M, Kehoe S, Kumar L, Friedlander M. Cancer of the ovary, fallopian tube, and peritoneum: 2021 update. *Int J Gynaecol Obstet.* 2021;155(Suppl 1):61–85.
- Harter P, Sehouli J, Reuss A, Hasenburger A, Scambia G, Cibula D, et al. Prospective validation study of a predictive score for operability of recurrent ovarian cancer: the Multicenter Intergroup Study DESKTOP II. A project of the AGO Kommission OVAR, AGO Study Group, NOGGO, AGO-Austria, and MITO. *Int J Gynecol Cancer.* 2011;21:289–95.
- Westergaard MCW, Milne K, Pedersen M, Hasselager T, Olsen LR, Anglesio MS, et al. Changes in the tumor immune microenvironment during disease progression in patients with ovarian cancer. *Cancers (Basel).* 2020;12:3828.
- Kreuzinger C, Geroldinger A, Smeets D, Braicu EI, Sehouli J, Koller J, et al. A complex network of tumor microenvironment in human high-grade serous ovarian cancer. *Clin Cancer Res.* 2017;23:7621–32.
- Patch AM, Christie EL, Etemadmoghadam D, Garsed DW, George J, Fereday S, et al. Whole-genome characterization of chemoresistant ovarian cancer. *Nature.* 2015;521:489–94.
- Cancer Genome Atlas Research N. Integrated genomic analyses of ovarian carcinoma. *Nature.* 2011;474:609–15.
- Lisio MA, Fu L, Goyeneche A, Gao ZH, Telleria C. High-grade serous ovarian cancer: basic sciences, clinical and therapeutic standpoints. *Int J Mol Sci.* 2019;20:952.
- Ojalvo LS, Thompson ED, Wang TL, Meeker AK, Shih IM, Fader AN, et al. Tumor-associated macrophages and the tumor immune microenvironment of primary and recurrent epithelial ovarian cancer. *Hum Pathol.* 2018;74:135–47.
- Stanske M, Wienert S, Castillo-Tong DC, Kreuzinger C, Vergote I, Lambrechts S, et al. Dynamics of the intratumoral immune response during progression of high-grade serous ovarian cancer. *Neoplasia.* 2018;20:280–8.
- Ruscito I, Cacsire Castillo-Tong D, Vergote I, Ignat I, Stanske M, Vanderstichele A, et al. Characterisation of tumour microvessel density during progression of high-grade serous ovarian cancer: clinico-pathological impact (an OCTIPS Consortium study). *Br J Cancer.* 2018;119:330–8.
- Kobel M, Piskorz AM, Lee S, Lui S, LePage C, Marass F, et al. Optimized p53 immunohistochemistry is an accurate predictor of TP53 mutation in ovarian carcinoma. *J Pathol Clin Res.* 2016;2:247–58.

15. Denkert C, Romey M, Swedlund B, Hattesoehl A, Teply-Szymanski J, Kommos S, et al. Homologous recombination deficiency as an ovarian cancer biomarker in a real-world cohort: validation of decentralized genomic profiling. *J Mol Diagn.* 2022;24:1254–63.
16. Willing EM, Vollbrecht C, Vossing C, Weist P, Schallenberg S, Herbst JM, et al. Development of the NOGGO GIS v1 assay, a comprehensive hybrid-capture-based NGS assay for therapeutic stratification of homologous repair deficiency driven tumors and clinical validation. *Cancers (Basel).* 2023;15:3445.
17. Uhlen M, Fagerberg L, Hallstrom BM, Lindskog C, Oksvold P, Mardinoglu A, et al. Proteomics. Tissue-based map of the human proteome. *Science.* 2015;347:1260419.
18. Dragomir MP, Calina TG, Perez E, Schallenberg S, Chen M, Albrecht T, et al. DNA methylation-based classifier differentiates intrahepatic pancreato-biliary tumours. *EBioMedicine.* 2023;93:104657.
19. Aryee MJ, Jaffe AE, Corrada-Bravo H, Ladd-Acosta C, Feinberg AP, Hansen KD, et al. Minfi: a flexible and comprehensive Bioconductor package for the analysis of Infinium DNA methylation microarrays. *Bioinformatics.* 2014;30:1363–9.
20. Fortin JP, Triche TJ Jr., Hansen KD. Preprocessing, normalization and integration of the Illumina HumanMethylationEPIC array with minfi. *Bioinformatics.* 2017;33:558–60.
21. Fortin JP, Labbe A, Lemire M, Zanke BW, Hudson TJ, Fertig EJ, et al. Functional normalization of 450k methylation array data improves replication in large cancer studies. *Genome Biol.* 2014;15:503.
22. Teschendorff AE, Marabita F, Lechner M, Bartlett T, Tegner J, Gomez-Cabrero D, et al. A beta-mixture quantile normalization method for correcting probe design bias in Illumina Infinium 450 k DNA methylation data. *Bioinformatics.* 2013;29:189–96.
23. Demichev V, Messner CB, Vernardis SI, Lilley KS, Ralser M. DIA-NN: neural networks and interference correction enable deep proteome coverage in high throughput. *Nat Methods.* 2020;17:41–44.
24. Budczies J, Klauschen F, Sinn BV, Gyorffy B, Schmitt WD, Darb-Esfahani S, et al. Cutoff finder: a comprehensive and straightforward Web application enabling rapid biomarker cutoff optimization. *PLoS ONE.* 2012;7:e51862.
25. Gyorffy B, Lanczky A, Szallasi Z. Implementing an online tool for genome-wide validation of survival-associated biomarkers in ovarian-cancer using microarray data from 1287 patients. *Endocr Relat Cancer.* 2012;19:197–208.
26. Di Palma T, Lucci V, de Cristofaro T, Filippone MG, Zannini M. A role for PAX8 in the tumorigenic phenotype of ovarian cancer cells. *BMC Cancer.* 2014;14:292.
27. Zudaire E, Cuesta N, Murty V, Woodson K, Adams L, Gonzalez N, et al. The aryl hydrocarbon receptor repressor is a putative tumor suppressor gene in multiple human cancers. *J Clin Invest.* 2008;118:640–50.
28. Jung YS, Park JI. Wnt signaling in cancer: therapeutic targeting of Wnt signaling beyond beta-catenin and the destruction complex. *Exp Mol Med.* 2020;52:183–91.
29. Kawano Y, Kypka R. Secreted antagonists of the Wnt signalling pathway. *J Cell Sci.* 2003;116:2627–34. (Pt 13)
30. Liu Y, Zhou Q, Zhou D, Huang C, Meng X, Li J. Secreted frizzled-related protein 2-mediated cancer events: Friend or foe? *Pharm Rep.* 2017;69:403–8.
31. Lustig B, Jerchow B, Sachs M, Weiler S, Pietsch T, Karsten U, et al. Negative feedback loop of Wnt signaling through upregulation of conductin/axin2 in colorectal and liver tumors. *Mol Cell Biol.* 2002;22:1184–93.
32. Uysal-Onganer P, Kypka RM. Wnt11 in 2011—the regulation and function of a non-canonical Wnt. *Acta Physiol (Oxf).* 2012;204:52–64.
33. Li B, Cai S, Zhao Y, He Q, Yu X, Cheng L, et al. Nerve growth factor modulates the tumor cells migration in ovarian cancer through the WNT/beta-catenin pathway. *Oncotarget.* 2016;7:81026–48.
34. Leung YK, Lau KM, Mobley J, Jiang Z, Ho SM. Overexpression of cytochrome P450 1A1 and its novel spliced variant in ovarian cancer cells: alternative subcellular enzyme compartmentation may contribute to carcinogenesis. *Cancer Res.* 2005;65:3726–34.
35. Aust S, Felix S, Auer K, Bachmayr-Heyda A, Kenner L, Dekan S, et al. Absence of PD-L1 on tumor cells is associated with reduced MHC I expression and PD-L1 expression increases in recurrent serous ovarian cancer. *Sci Rep.* 2017;7:42929.
36. Vogel CFA, Haarmann-Stemmann T. The aryl hydrocarbon receptor repressor—more than a simple feedback inhibitor of AhR signaling: Clues for its role in inflammation and cancer. *Curr Opin Toxicol.* 2017;2:109–19.
37. Mimura J, Ema M, Sogawa K, Fujii-Kuriyama Y. Identification of a novel mechanism of regulation of Ah (dioxin) receptor function. *Genes Dev.* 1999;13:20–25.
38. Feng S, Cao Z, Wang X. Role of aryl hydrocarbon receptor in cancer. *Biochim Biophys Acta.* 2013;1836:197–210.
39. Opitz CA, Litznerburger UM, Sahm F, Ott M, Tritschler I, Trump S, et al. An endogenous tumour-promoting ligand of the human aryl hydrocarbon receptor. *Nature.* 2011;478:197–203.
40. Ikuta T, Kawajiri K. Zinc finger transcription factor Slug is a novel target gene of aryl hydrocarbon receptor. *Exp Cell Res.* 2006;312:3585–94.
41. Donovan MG, Selmin OL, Doetschman TC, Romagnolo DF. Epigenetic activation of BRCA1 by Genistein in vivo and triple negative breast cancer cells linked to antagonism toward aryl hydrocarbon receptor. *Nutrients.* 2019;11:2559.
42. Deuster E, Mayr D, Hester A, Kolben T, Zeder-Goss C, Burges A, et al. Correlation of the aryl hydrocarbon receptor with FSHR in ovarian cancer patients. *Int J Mol Sci.* 2019;20:2862.
43. Su KM, Gao HW, Chang CM, Lu KH, Yu MH, Lin YH, et al. Synergistic AHR binding pathway with EMT effects on serous ovarian tumors recognized by multi-disciplinary integrated analysis. *Biomedicine.* 2021;9:866.
44. Vogel CFA, Lazennec G, Kado SY, Dahlem C, He Y, Castaneda A, et al. Targeting the aryl hydrocarbon receptor signaling pathway in breast cancer development. *Front Immunol.* 2021;12:625346.
45. Vacher S, Castagnet P, Chemlali W, Lallemand F, Meseure D, Pocard M, et al. High AHR expression in breast tumors correlates with expression of genes from several signaling pathways namely inflammation and endogenous tryptophan metabolism. *PLoS ONE.* 2018;13:e0190619.
46. Cain JA, Montibus B, Oakey RJ. Intragenic CpG islands and their impact on gene regulation. *Front Cell Dev Biol.* 2022;10:832348.
47. Xiao X, Xiao Y, Wen R, Zhang Y, Li X, Wang H, et al. Promoting roles of the secreted frizzled-related protein 2 as a Wnt agonist in lung cancer cells. *Oncol Rep.* 2015;34:2259–66.
48. Roth W, Wild-Bode C, Platten M, Grimm C, Melkonyan HS, Dichgans J, et al. Secreted frizzled-related proteins inhibit motility and promote growth of human malignant glioma cells. *Oncogene.* 2000;19:4210–20.
49. Kasashima H, Duran A, Martinez-Ordonez A, Nakanishi Y, Kinoshita H, Linares JF, et al. Stromal SOX2 upregulation promotes tumorigenesis through the generation of a SFRP1/2-expressing cancer-associated fibroblast population. *Dev Cell.* 2021;56:95–110 e110.
50. Mariani A, Wang C, Ober AL, Riska SM, Torres M, Kumka J, et al. Genes associated with bowel metastases in ovarian cancer. *Gynecol Oncol.* 2019;154:495–504.
51. Arend RC, Londono AI, Montgomery AM, Smith HJ, Dobbin ZC, Katre AA, et al. Molecular response to neoadjuvant chemotherapy in high-grade serous ovarian carcinoma. *Mol Cancer Res.* 2018;16:813–24.
52. Javellana M, Eckert MA, Heide J, Zawieracz K, Weigert M, Ashley S, et al. Neoadjuvant chemotherapy induces genomic and transcriptomic changes in ovarian cancer. *Cancer Res.* 2022;82:169–76.
53. Yuan H, Yu Q, Pang J, Chen Y, Sheng M, Tang W. The value of the stemness index in ovarian cancer prognosis. *Genes (Basel).* 2022;13:993.
54. Su HY, Lai HC, Lin YW, Chou YC, Liu CY, Yu MH. An epigenetic marker panel for screening and prognostic prediction of ovarian cancer. *Int J Cancer.* 2009;124:387–93.
55. Niskakoski A, Kaur S, Staff S, Renkonen-Sinisalo L, Lassus H, Jarvinen HJ, et al. Epigenetic analysis of sporadic and Lynch-associated ovarian cancers reveals histology-specific patterns of DNA methylation. *Epigenetics.* 2014;9:1577–87.
56. Al-Shabanah OA, Hafez MM, Hassan ZK, Sayed-Ahmed MM, Abozeid WN, Alsheikh A, et al. Methylation of SFRPs and APC genes in ovarian cancer infected with high risk human papillomavirus. *Asian Pac J Cancer Prev.* 2014;15:2719–25.
57. Duan H, Yan Z, Chen W, Wu Y, Han J, Guo H, et al. TET1 inhibits EMT of ovarian cancer cells through activating Wnt/beta-catenin signaling inhibitors DKK1 and SFRP2. *Gynecol Oncol.* 2017;147:408–17.
58. Schwede M, Waldron L, Mok SC, Wei W, Basunia A, Merritt MA, et al. The impact of stroma admixture on molecular subtypes and prognostic gene signatures in serous ovarian cancer. *Cancer Epidemiol Biomark Prev.* 2020;29:509–19.

## ACKNOWLEDGEMENTS

We want to thank Sylwia Handzik, Birgit Schaefer and Ines Koch for their great technical assistance and HTG Molecular Inc. for their kind support, providing us with two chips (for 24 patient samples each) for a pilot examination. We are furthermore thankful to members of the Institute of Biometry and Clinical Epidemiology (Charité Berlin) for their statistical advice. This work was financially supported by the TRANSCAN-2 project (grant no.:2014-121) funded by the European Commission under the EU framework program Horizon2020 (grant agreement 643638) and by Berliner Krebsgesellschaft (DRFF202204 to M.P.D.). We also acknowledge support to C.S. from the MESI-STRAT project (grant agreement 754688). T.S. was funded by the Deutsche Forschungsgemeinschaft (DFG, German Research Foundation) –RTG2424/CompCancer – project number: 377984878. M.P.D. is supported by Berlin Institute of Health, Junior Clinician Scientist Program and by a DTK Berlin Young Investigator Grant 2022. A.M. and F.C. acknowledge funding by the Federal Ministry of Education and Research (BMBF), as part of the National Research Initiatives for Mass Spectrometry in Systems Medicine, under grant agreement no. 161L0222. K.K. acknowledges the support of the Stiftung Charité through the Private Excellence Initiative Johanna Quandt and the Josette Renée Bissinger Legacy Fund.

## AUTHOR CONTRIBUTIONS

NM, MPD, CS and ETT performed study concept and design; NM, MPD, BVS, CS and ETT performed writing, review and revision of the paper; NM, MPD performed experiments; A.M. performed mass spectrometry-based proteomics, data analysis and interpretation, under supervision of FC; BVS, CAK., WDS, JP, IP, DH, JS, EIB, CD, SDE and ETT provided patient acquisition and tissue collection; NM, MPD, BVS, IH, AM, TS, TGC, KK, DC, FC, MM, CS, ETT provided analysis and interpretation of data, and statistical analysis; IH, IP, JI, FT, SM, C Keunecke, C Kreuzinger, DCC-T and HK provided methodical support. All authors read and approved the final paper.

## FUNDING

Open Access funding enabled and organized by Projekt DEAL.

## COMPETING INTERESTS

The authors declare no competing interests.

## ETHICS APPROVAL AND CONSENT TO PARTICIPATE

The collection of tissue from Charité Universitätsmedizin Berlin was processed according to the Charité ethics vote EA1/051/18 and EA1/110/22. As anonymized tissue samples were used retrospectively, the need to obtain informed consent was waived. The study was performed in accordance with the Declaration of Helsinki.

## ADDITIONAL INFORMATION

**Supplementary information** The online version contains supplementary material available at <https://doi.org/10.1038/s41416-023-02550-1>.

**Correspondence** and requests for materials should be addressed to Eliane T. Taube.

**Reprints and permission information** is available at <http://www.nature.com/reprints>

**Publisher's note** Springer Nature remains neutral with regard to jurisdictional claims in published maps and institutional affiliations.



**Open Access** This article is licensed under a Creative Commons Attribution 4.0 International License, which permits use, sharing, adaptation, distribution and reproduction in any medium or format, as long as you give appropriate credit to the original author(s) and the source, provide a link to the Creative Commons licence, and indicate if changes were made. The images or other third party material in this article are included in the article's Creative Commons licence, unless indicated otherwise in a credit line to the material. If material is not included in the article's Creative Commons licence and your intended use is not permitted by statutory regulation or exceeds the permitted use, you will need to obtain permission directly from the copyright holder. To view a copy of this licence, visit <http://creativecommons.org/licenses/by/4.0/>.

© The Author(s) 2024